In-Place Modulation of Rectification in Tunneling Junctions Comprising Self-Assembled Monolayers

Ai, Yong; Kovalchuk, Andrii; Qiu, Xinkai; Zhang, Yanxi; Kumar, Sumit; Wang, Xintai; Kühnel, Martin; Nørgaard, Kasper; Chiechi, Ryan C

Published in:
Nano Letters

DOI:
10.1021/acs.nanolett.8b03042

Publication date:
2018

NANO LETTERS

Letter

Cite This: Nano Lett. 2018, 18, 7552−7559

pubs.acs.org/NanoLett

In-Place Modulation of Rectification in Tunneling Junctions Comprising Self-Assembled Monolayers

Yong Ai,[†,‡] Andrii Kovalchuk,[†,‡] Xinkai Qiu,[†,‡] Yanxi Zhang,[†,‡] Sumit Kumar,[†,‡] Xintai Wang,[§] Martin Kühnel,[§] Kasper Nørgaard,[§] and Ryan C. Chiechi*[,†,‡]

[†]Stratingh Institute for Chemistry, University of Groningen, Nijenborgh 4, 9747 AG Groningen, The Netherlands

[‡]Zernike Institute for Advanced Materials, Nijenborgh 4, 9747 AG Groningen, The Netherlands

[§]Nano-Science Center & Department of Chemistry, University of Copenhagen, Universitetsparken 5, DK-2100 Copenhagen, Denmark

Supporting Information

ABSTRACT: This paper describes tunneling junctions comprising self-assembled monolayers that can be converted between resistor and diode functionality in-place. The rectification ratio is affected by the hydration of densely packed carboxylic acid groups at the interface between the top-contact and the monolayer. We studied this process by treatment with water and a water scavenger using three different top-contacts, eutectic Ga−In (EGaIn), conducting-probe atomic force microscopy (CP-AFM), and reduced graphene oxide (rGO), demonstrating that the phenomena is molecular in nature and is not platform-speciffc. We propose a mechanism in which the tunneling junctions convert to diode behavior through the lowering of the LUMO, which is suffcient to bring it close to resonance at positive bias, potentially assisted by a Stark shift. This shift in energy is supported by calculations and a change in polarization observed by X-ray photoelectron spectroscopy and Kelvin probe measurements. We demonstrate light-driven modulation using spiropyran as a photoacid, suggesting that any chemical process that is coupled to the release of small molecules that can tightly bind carboxylic acid groups can be used as an external stimulus to modulate rectification. The ability to convert a tunneling junction reversibly between a diode and a resistor via an effect that is intrinsic to the molecules in the junction extends the possible applications of Molecular Electronics to reconfigurable circuits and other new functionalities that do not have direct analogs in conventional semiconductor devices.

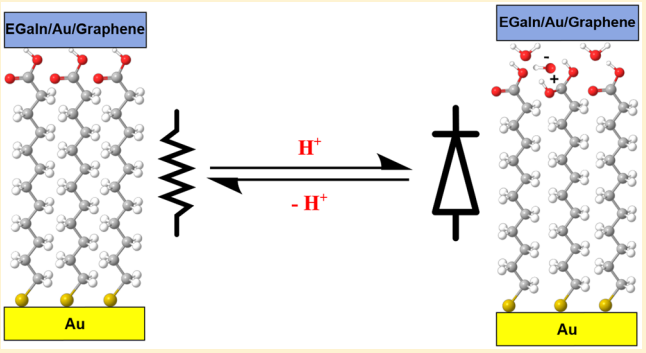

KEYWORDS: *Rectification, molecular diode, EGaIn, graphene, self-assembled monolayers*

Modern information technology relies on computational platforms across a broad range of length-scales from embedded, Internet of Things devices to personal, mobile devices to supercomputing clusters to data centers. These platforms increasingly demand specialized electronics suited to a particular application, e.g., low-power and neuromorphic chips.[1] Molecular electronics (the transport of charge through molecules spanning two or more electrodes) has tremendous potential for specialized computation because changes at the Ångstrom-scale can translate into exponential effects at the device level.[2] And because the functional units are molecules, these effects can arise from chemical phenomena like photoisomerization.[3,4] Molecular diodes, the basis of logic circuits,[5] are now well established in both single-molecule junctions[6] and devices[7] comprising self-assembled monolayers (SAMs) with eutectic Ga−In (EGaIn) top-contacts.[8] However, the realization of new concepts in computation requires new functionality that exploits the chemical nature of molecular electronics.

This paper describes the reversible interconversion of molecular tunneling junctions comprising SAMs between diodes and resistors. The molecules in the SAM are terminated by carboxylic groups (CO_2H), which, when densely packed, can bind water tightly, affecting surface states in the SAM and the electronic structure of the molecules therein, hence the current density vs voltage (J/V) characteristics. The rectification ratio, $R = |J(V^+)/J(V^-)|$, of tunneling junctions comprising SAMs is highly sensitive both to the structure of the SAM and to the molecules in the SAM and can be tuned synthetically, i.e., by comparing R between junctions formed from structurally similar SAMs.[9,10] Rectification can also be induced by breaking the symmetry of electrodes in an electrochemical (ionic) environment.[11] However, these approaches cannot produce a junction whose function can

Received: July 25, 2018
Revised: September 27, 2018
Published: November 6, 2018

DOI: 10.1021/acs.nanolett.8b03042
Nano Lett. 2018, 18, 7552−7559

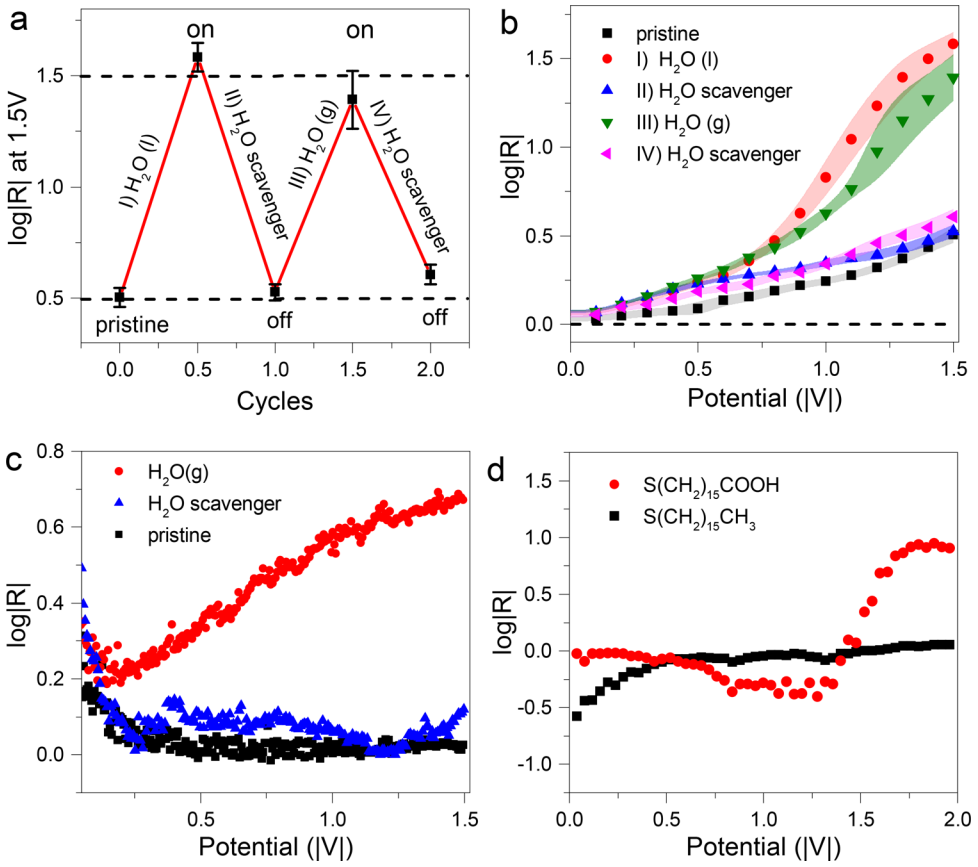

Figure 1. In-place modulation of the rectification of junctions comprising SAMs of $S(CH_2)_{11}CO_2H$. (a) log|*R*| at 1.5 V versus H_2O/2,2-dimethoxypropane exposure cycles for $Au^{TS}/S(CH_2)_{11}CO_2H//EGaIn$ junctions. (b) Semilog plots of the rectification ratio (log|*R*|) versus absolute potential (|*V*|) for $Au^{TS}/S(CH_2)_{11}CO_2H//EGaIn$ junctions before and after the SAMs are treated with H_2O or H_2O and then DMP. Black, pristine, as-prepared; red, after exposure to H_2O (l); blue, after exposure to H_2O (l) and then DMP; green, after exposure to H_2O (g); magenta, after exposure to H_2O (g) and then DMP. (c) Plots of log|*R*| versus |*V*| for $Au^{TS}/S(CH_2)_{11}CO_2H//Au^{AFM}$ junctions after the SAMs are treated with H_2O or H_2O and then DMP. black, pristine; red, after exposure to H_2O (g); blue, after exposure to H_2O (g) and then DMP. (d) Plots of log|*R*| versus |*V*| for $Au^{VD}/S(CH_2)_{15}CH_3//rGO$ (black) and $Au^{VD}/S(CH_2)_{15}CO_2H//rGO$ (red) junctions.

be changed in-place because they rely either on comparing different SAMs or different environments around a transient single-molecule junction. And, while it is possible to affect *R* by altering the relative humidity,[12] the state of the junction depends on the environment surrounding the experimental setup during measurement; the value of *R* is, therefore, transient and specific to one experimental platform. Similarly, both *R* and conductance can be affected by changes to the hydration state of specific substrates supporting monolayers.[13] However, because we alter the properties of the SAM in-place and independently of the experimental platform, electrodes, and the conditions under which the junctions are measured, a junction can be converted between diode and a resistor behavior by switching the SAM itself between persistent rectifying and nonrectifying states. Moreover, through the use of a photoacid, we demonstrate that this process can be coupled to light and, therefore, any extrinsic phenomenon that generates (or absorbs) free protons.

Results and Discussion. *Electrical Measurements.* We followed literature procedures for forming high-quality SAMs of long-chain ω-thiol carboxylic acids, which require care to avoid the formation of bilayers and internally hydrogen-bonded structures.[14] To ensure that the resulting SAMs are fully protonated, we grew the SAMs in dry ethanol (EtOH) and compared them to SAMs grown in EtOH acidified with acetic acid[15] and found no difference in the *J*/*V* characteristics. We grew the SAMs on either template-stripped[16] Au (Au^{TS}) or vapor deposited Au (Au^{VD}) and formed Au^{TS}/SAM//EGaIn, Au^{TS}/SAM//Au^{AFM}, and Au^{VD}/SAM //rGO junctions where "/" and "//" denote covalent and van der Waals contacts, respectively, Au^{AFM} is a gold-coated atomic force microscopy (AFM) tip, and rGO is reduced graphene oxide.[17] Using EGaIn and Au^{AFM} top-contacts, we altered the *J*/*V* characteristics from the as-prepared, nonrectifying (resistor) to the rectifying (diode) state by exposure to water or a photoacid and back to the nonrectifying state using 2,2-dimethoxypropane (DMP) as a water scavenger[18] or NaOH in EtOH as an anhydrous base. In the presence of catalytic acid (e.g., RCO_2H) DMP reactions quantitatively with water to form acetone and methanol. The junctions are stable in both states; exposure to ambient conditions does not increase *R* over time and exposure to high vacuum (down to 1×10^{-8} mbar) or heating to 80 °C in moderate vacuum does not decrease it (Figure S2).

Figure 1a shows the value of log|*R*| over two complete cycles of alternating exposure to H_2O and DMP, and Figure 1b shows semilog plots of log|*R*| vs potential (*R*/*V*) curves of $Au^{TS}/S(CH_2)_{11}CO_2H//EGaIn$ junctions. Each value of log|*R*| is the peak of a Gaussian fit to a histogram of log|*R*| for that value of |*V*|, and the shaded areas are the 99% confidence intervals.

DOI: 10.1021/acs.nanolett.8b03042
Nano Lett. 2018, 18, 7552−7559

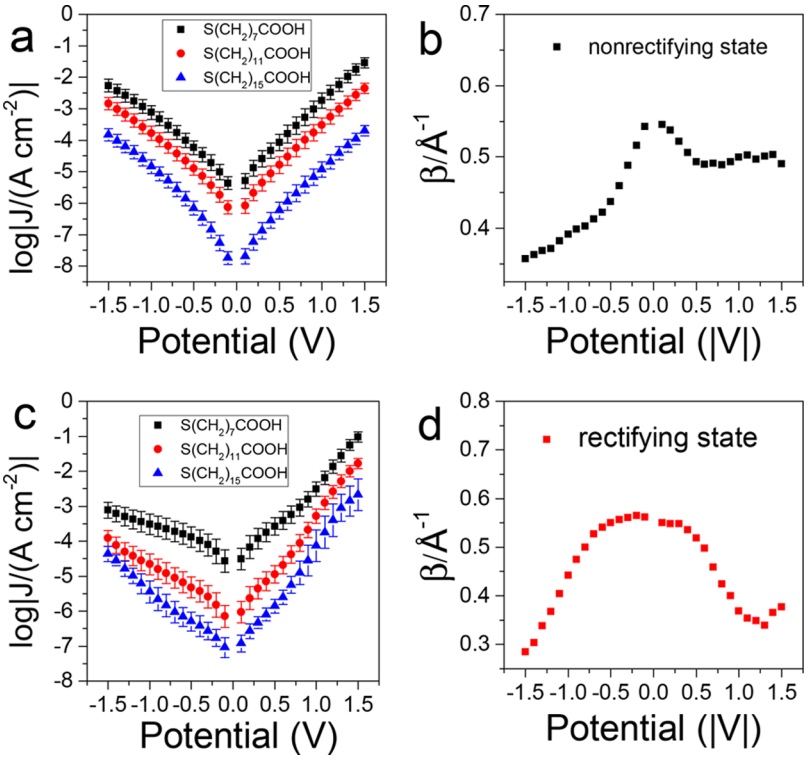

Figure 2. Plots of ln|*J*| versus |*V*| of $Au^{TS}/S(CH_2)_nCO_2H//EGaIn$ junctions where n = 7, 11, 15 in the nonrectifying (a) and rectifying (c) states. The tunneling decay coefficient, β, extracted from fits of ln|*J*| versus molecular length (Å) show a weak, approximately symmetric voltage dependence in the nonrectifying (b) and rectifying (d) state.

These measurements were performed inside a flowbox with 1−3% O_2 in N_2 and relative humidity (RH) < 10%.[19] (The presence of O_2 is necessary to form tips of EGaIn.) It is possible that the nonzero RH induces the small degree of rectification in the as-prepared SAMs (the dashed line in Figure 1b shows a perfect resistor, log|*R*| = 0) or that the asymmetric nature of $Au^{TS}/S(CH_2)_{11}CO_2H//EGaIn$ junctions introduces a slight asymmetry in the *J*/*V* characteristics.[7] However, after exposure to H_2O (vapor or liquid), increases exponentially with |*V*|. (We reiterate that the SAMs are grown in rigorously anhydrous conditions and are always measured under controlled and invariant conditions; the exposure to H_2O alters the intrinsic properties of the SAM and occurs completely spatially and temporally separate from the measurement.) An obvious explanation for the increase in log|*R*| is that H_2O in the junction undergoes redox chemistry and the *R*/*V* dependence is simply a reflection of the different oxidation reduction potentials; however, that behavior is both time-dependent and hysteretic,[20] neither of which is true for the junctions we measured (Figure S4). Moreover, subsequent exposure to a 1:1 by volume solution of DMP in ethanol returns the *R*/*V* curve to the pristine, nonrectifying state, which is a clear indication that no irreversible processes occur during *J*/*V* cycling in the rectifying state (i.e., after exposure to H_2O). We hypothesize that the primary cause of the dampening is mechanical stress to the SAM from repeated exposure to H_2O and DMP between measurements. Although the magnitude of the change in *R* dampens, the fact that the junctions survive multiple cycles proves that the underlying mechanism is inherently reversible and can therefore likely be improved with better molecular design and junction/device optimizations. Moreover, the magnitude of log|*R*| is already among the higher values reported (Figure S3).

The rate of tunneling charge transport through $S(CH_2)_{15}CH_3$ (C16) and oligophenyleneethynylene junctions is sensitive to both ambient humidity and exposure H_2O (g), which affects the height of the tunneling barrier.[21,22] However, exposure to H_2O (g) and/or H_2O (l) does not affect log|*R*| for $Au^{TS}/SAM//EGaIn$ junctions comprising C16 or $S(CH_2)_{11}CH_3$ (Figure S5). The simplest, most robust, and widely accepted measure of the barrier height of a tunneling junction is the tunneling decay coefficient, β, which is extracted from $J = J_0 e^{-\beta d}$ where d is the barrier width and J_0 is the theoretical value of J when $d = 0$. Although the rate of tunneling and the details of the energy landscape within a tunneling junction depend on many factors, β is defined only by the average height of the tunneling barrier ϕ and the constants $\hbar$ and m; $\beta = 2\hbar^{-1}\sqrt{2m\phi}$. Thus, the magnitude of β directly reflects the difference in energy between the Fermi level E_f and the most accessible molecular orbital, and if the change in *R* were the result of changes to molecular orbital states or symmetry (as is the case in ref 12), β would differ in the nonrectifying and rectifying states.

We determined β for the series $\{S(CH_2)_7CO_2H$, $S(CH_2)_{11}CO_2H$, $S(CH_2)_{15}CO_2H\}$ in the nonrectifying and rectifying states (by exposure to H_2O (g), Figure 2). The low-bias value of $\beta = 0.55^{-1}$ is lower than the consensus value of 0.70 $Å^{-1}$ for SAMs of alkanethiolates,[23−25] but it does not differ significantly between the nonrectifying and rectifying states, indicating that the mechanism of rectification does not involve changing the average barrier height that is imposed by the aliphatic molecular backbone. Thus, the effects of exposure to H_2O are likely confined to the SAM//top-contact interface via strong interactions between the terminal CO_2H groups and H_2O, which is supported spectroscopically (see below) and by

DOI: 10.1021/acs.nanolett.8b03042
Nano Lett. 2018, 18, 7552−7559

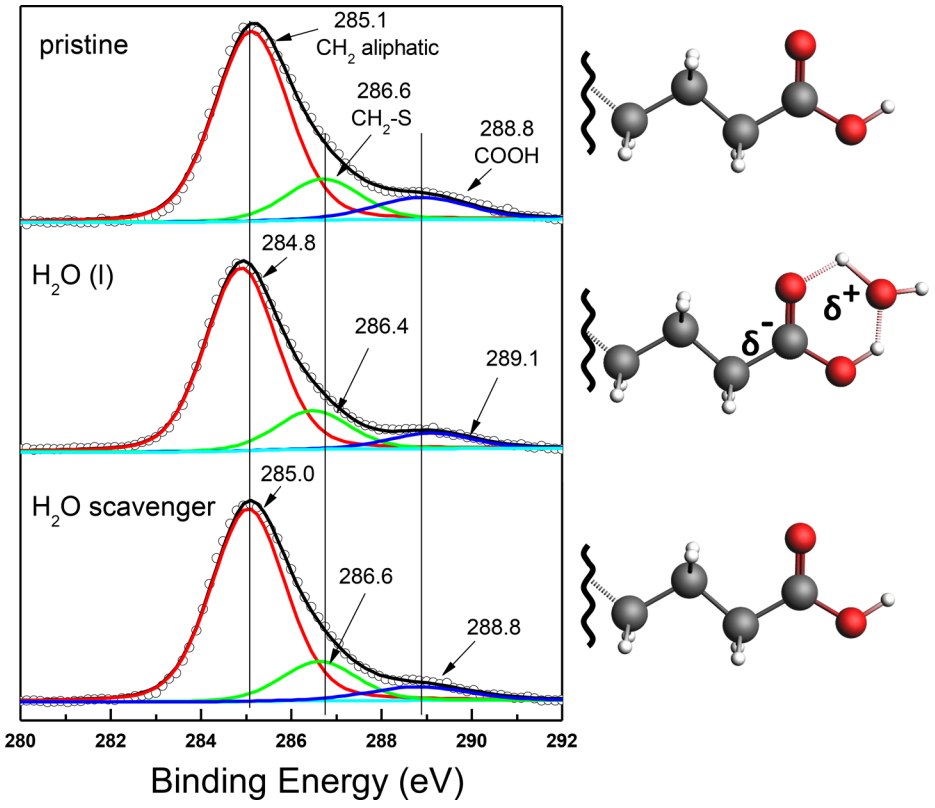

Figure 3. C 1s core X-ray photoemission spectra of SAMs of $S(CH_2)_{11}CO_2H$ before and after exposure to H_2O and H_2O subsequent treatment with DMP. Top: C 1s core-level region of a pristine SAM showing three main peaks located at 285.1, 286.6, and 288.8 eV, corresponding to CH_2 aliphatic, CH_2−S, and CO_2H, respectively. Center: After exposure to H_2O (l), the CO_2H peak shifts 0.3 eV to higher binding energy while the CH_2 aliphatic and CH_2−S peaks shift 0.3 eV to lower binding energy. Bottom: After exposure to H_2O and then DMP, the three main C 1s peaks shift back to their initial position with respect to the pristine state.

the observation that H_2O does not desorb in vacuum with heating (Figure S2).

It is possible to induce rectification (with symmetric molecules) in molecular tunneling junctions by altering the electric double layer of the electrodes such that they experience different electrostatic environments.[11] This mechanism is plausible, as EGaIn forms a 7 Å thick layer of Ga_2O_3 that should interact strongly with both carboxylic acids and water.[26] However, Figure 1c shows R/V curves for $Au^{TS}S/(CH_2)_{11}CO_2H//Au^{AFM}$ junctions, which exhibit the same behavior as $Au^{TS}/S(CH_2)_{11}CO_2H//EGaIn$ junctions; as-prepared SAMs do not rectify until exposed to H_2O (l) and they return to their initial state upon exposure to DMP. A mechanism that depends on the electrodes should show markedly different behavior between dissimilar Au^{TS}/EGaIn and nearly identical Au^{TS}/Au^{AFM} pairs of electrodes. To exclude electrode effects completely, we measured $Au^{TS}/S(CH_2)_{15}CO_2H//rGO$ junctions; however, without in situ access to the SAM, we compared the rectifying state (because the devices are prepared in a water bath) to $Au^{TS}/S(CH_2)_{15}CH_3//rGO$ junctions. Figure 1d shows an abrupt increase in log|R| around 1.5 for the CO_2H-terminated SAMs that is absent for the alkane SAMs. Thus, the effect is entirely molecular and independent of the identity and composition of the electrodes. This is an important observation, as it means that the underlying mechanism of rectification switching is generalizable and can be utilized in any present or future device platform.

Mechanism of Rectification. For insight into the influence of bound water on the electronic structure of the SAMs, we characterized SAMs of $S(CH_2)_{11}CO_2H$ by X-ray photoelectron spectroscopy (XPS) in the pristine state, after exposure to water, and after subsequent treatment with DMP. These data are summarized in Figure 3. The three main peaks in the C1*s* core-level region correspond to aliphatic CH_2−CH_2, CH_2−S, and CO_2H carbons.[27,28] The binding energies associated with these carbons in both the pristine and DMP-treated SAMs (i.e., the nonrectifying sates) are 285.1 eV, 286.6 and 288.8 eV, respectively. In the C 1s spectra of the SAMs in the rectifying state (i.e., after exposure to H_2O, but before DMP treatment), the CO_2H peak shifts to a higher binding energy by 0.3 eV, suggesting that the CO_2H group becomes more electropositive when complexed with water.[27,39] Simultaneously, the aliphatic CH_2−CH_2 and CH_2−S peaks shift to lower binding energies by 0.3 and 0.2 eV, which indicates that the SAM becomes polarized when water binds. Kelvin-probe AFM (KPFM) shows that the work function of SAMs of $S(CH_2)_{11}CO_2H$ is approximately 600 meV higher than that of their $S(CH_2)_{11}CH_3$ alkane analogues and confirms the increased polarization at the CO_2H terminus of the SAM when water binds, which shifts it higher by approximately an additional 135 meV (Figure S9). This increase in polarization may also explain the small differences in the bias-dependence of β (Figure 2) between the rectifying and nonrectifying states.

Although the shifts in binding energies are small, they are within the resolution of the instrument and are reproducible and the Au 4f peaks are invariant (see Figure S1 and related

DOI: 10.1021/acs.nanolett.8b03042
Nano Lett. 2018, 18, 7552−7559

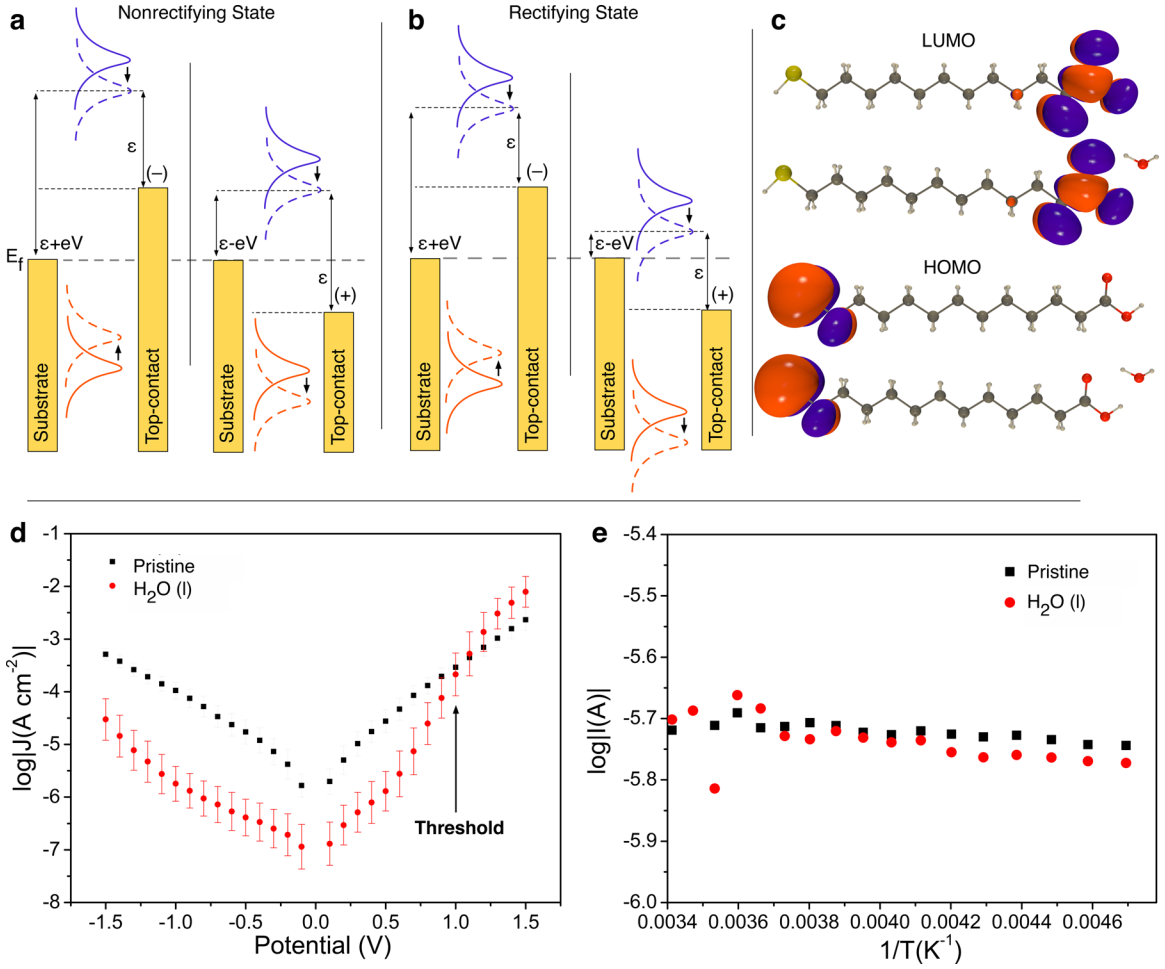

Figure 4. Proposed mechanism of rectification. Frontier orbitals are depicted as purple (LUMO) and orange (HOMO) Lorentzians. Solid lines indicate the relative positions when the vacuum level is shifted by the applied field. Dashed lines depict the direction of the Stark shift according to ab initio OVGF calculations (seethe Supporting Information). The Fermi level of the substrate is indicated as E_f, and the offset between the peak of the orbitals and the electrodes is indicated by ε, which is shifted by an amount eV at the grounded electrode. (a) In the nonrectifying (resistor) state, both frontier orbtials are relatively far from E_f, resulting in symmetric J/V curves within the accessible bias window. (b) In the rectifying (diode) state, the complexation of water creates a surface dipole that shifts the vacuum level in the same direction as positive bias, bringing the LUMO closer to E_f such that the tail can cross E_f at positive bias, giving rise to asymmetric J/V curves. (c) B3LYP/Def2QZVPP HOMO and LUMO orbitals of $HS(CH_2)_{11}CO_2H{\cdot}H_2O$. (d) Plots of log|$J$| versus applied bias ($V$) of $Au^{TS}/S(CH_2)_{11}COOH//EGaIn$ junctions in the pristine, nonrectifying (black squares) and rectifying (red circles) states. Each data point is the mean value from a Gaussian fit to a histogram of log|J| for a value of V. The error bars are the 95 confidence intervals of the fit. The J/V data are approximately symmetric in the nonrectifying state. After exposure to H_2O (l), log|J| decreases by approximately 1.5 until a threshold positive bias at which point it rises sharply, giving rise to rectification. (e) Plots of log|I| at 0.50 V as a function of inverse temperature for $Au^{TS}/S(CH_2)_{15}CO_2H//EGaIn$ junctions in the pristine, nonrectifying state (black squares) and rectifying state (red circles) suggesting the absence of thermally activated processes.

discussion in the Supporting Information). Importantly, all three C 1s peaks return to the binding energies of the pristine state after exposure to H_2O and subsequent treatment with DMP, indicating that the effects of binding H_2O are chemically reversible. Thus, the dampening effect in Figure 1 is not due to irreversible chemical processes and is most likely physical stress that introduces disorder, pinholes, and so forth. This type of fatigue can be mitigated through the optimization or use of different device platforms[30,31] much more readily than chemical fatigue.

Based on the experimental data described above, we describe the SAMs in the rectifying state as being formally hydrated by water: $CO_2H{\cdot}H_2O$. This is an imperfect description because we cannot know the stoichiometry of the complexation in the SAM and solution-phase phenomena do not always directly map onto surface-chemistry phenomena. For example, exposing SAMs bearing terminal CO_2H groups to H_2O can form up to six monolayers[32] of H_2O. However, we would expect physisorbed water to promote electrochemical processes under bias for which, as described above, there is no evidence. Given that we dry the SAMs thoroughly after exposure to H_2O and only treatment with DMP is sufficient to restore the SAMs to the pristine, nonrectifying state, we propose that, in the rectifying state, the SAMs bear a (partial) monolayer of tightly bound H_2O, which is best described as $CO_2H{\cdot}H_2O$.

While it is possible that the dipoles arising from the polarization of the SAM directly lead to rectification,[33,34] the magnitude of log|R| suggests the involvement of frontier molecular orbitals.[35] The XPS and KPFM data show that the polarization of SAMs of $S(CH_2)_nCO_2H{\cdot}H_2O$ translates into a lowering of frontier orbitals both from the increased

DOI: 10.1021/acs.nanolett.8b03042
Nano Lett. 2018, 18, 7552−7559

electronegativity of the terminal CO_2H groups and the increased work function, i.e., binding H_2O lowers the absolute and relative energy of the LUMO. The direction of the rectification, $J(+V) > J(-V)$, implicates the LUMO as the dominant frontier orbital;[35,36] however, variable-temperature measurements reveal a lack of thermally activated processes (Figure 4e), thus we can exclude a tunneling-hopping mechanism.[37] Instead, we propose the mechanism shown in Figure 4, in which the binding of water to the carboxylic acid groups brings the LUMO sufficiently close to the Fermi level that its tail is brought into resonance with the bottom electrode at bias. This mechanism is consistent with the observation that rectification is conserved across electrode pairs of Au^{TS}/EGaIn, Au^{TS}/Au^{AFM}, and Au^{VD}/rGO. It is further supported by the observation that the conductance drops upon binding water, except at positive bias above a certain threshold; the binding of water increases the width of the tunneling barrier, decreasing the conductance until a threshold bias at which the tail of the LUMO crosses E_f (Figure 4b and d).

Given that the B3LYP/def2-TZVPP gas-phase energy of the LUMO of $S(CH_2)_{11}CO_2H{\cdot}H_2O$ is −0.06 eV, the expectation is that, at zero bias, the HOMO (−6.46 eV) would dominate tunneling charge-transport (at least in single-molecule junctions). Rectification, however, is observed in SAMs and at bias, which shifts the vacuum level and which can induce Stark shifts that alter the positions and energies of atomic and/or molecular orbitals in the presence of an electric field. Frisbie et al. recently examined the Stark effect in $Au/S(CH_2)_nCH_3//Au^{AFM}$ junctions, where n = 7,8,9,10,12, using ab initio outer-valence Greens function (OVGF) calculations.[38] They found a linear dependence of the energy of the HOMO on the applied field and an approximately parabolic dependence of the LUMO, centered around zero, concluding that transport is dominated by the HOMO, which tracks with the tip bias such that it moves closer to E_f at negative bias. The resulting asymmetry in the I/V data is very small because most of the voltage drops at the Au−S interface. We applied the same methodology to $HS(CH_2)_{11}CO_2H$ and $HS(CH_2)_{11}CO_2H{\cdot}H_2O$ to examine the influence of the additional molecular orbtials localized on the carboxylic acid group, finding the same dependence of the HOMO and LUMO on applied field (Figure S7). These shifts are depicted with dashed-line curves in Figure 4a and b, which either add to or subtract from the vacuum-level shift induced by the electric field. In the nonrectifying state, the LUMO does not play a substantial role (Figure 4a); however, the complexation of water makes the terminal CO_2H group more electropositive (Figures 3 and S9), lowering the LUMO and inducing a dipole moment at the surface that adds to the Stark shift at positive bias and subtracts from it at negative bias (Figures 4b and S7). The HOMO is localized at the thiol (and hybridized with the substrate), shifted down in energy with respect to its alkyl analogue, and its contribution to tunneling charge-transport is, therefore, small and constant in both states. Figure 4c shows isoplots of the frontier orbtials. The presence of H_2O does not affect the isoplots in these minimized geometries and, for single molecules in the gas phase, has a negligible impact on the energies of the orbitals, shifting them by only 0.08.eV.

Light-Driven Switching. Treatment with H_2O and DMP to affect R is a direct chemical input in that it requires physically exposing a SAM to either H_2O or a solution containing DMP. Photoacids trigger the release of acidic protons upon treatment with light. Thus, if protic species other than H_2O can also induce polarization at the CO_2H interface, it should be possible to affect R with light. For example, a photoacid dissolved in an alcohol produces equilibrium amounts of ROH_2^+, which could potentially serve as a proxy for H_2O to affect switching optically rather than physically.

To explore the role of H_2O in the polarization of CO_2H groups, we examined the influence of pH on log by $|R|$ treating the as-prepared SAMs with aqueous solutions of 1×10^{-4} M HCl, 1×10^{-4} M CH_3CO_2H, and 3% NH_4OH. All three induced rectifying behavior, while 1×10^{-4} M NaOH in anhydrous ethanol did not (Figure S6). This observation confirms that the SAMs bind H_2O irrespective of pH and that, upon removal from contact with water (vapor or liquid), they are polarized through strong interactions between CO_2H and H_2O. It also suggests that labile protons play an important role. The acid/base properties of SAMs bearing CO_2H groups is counterintuitive since the pK_a of free CO_2H groups is about 3−5; however, bulk dissociation constants do not directly inform the protonation/charge state of interfaces[39] and SAMs bearing CO_2H can be protonated by HCl in methanol, resulting in a positive ζ-potential.[29] When packed into a SAM, ΔG of (de)protonation is strongly affected by the van der Waals interactions between the alkane backbones and the intermolecular hydrogen bonding of the CO_2H groups; The effective pK_a of SAMs of carboxylic acids increases by up to 4 pK_a units and is sensitive to chain-lengths.[40] This behavior is due to the fact that protonation creates more hydrogen bonds while simultaneously causing Coulomb repulsion; the former is energetically favorable, while the latter becomes increasingly unfavorable as van der Waals interactions in the backbone are disrupted. That balance is why increasing the radius of curvature of nanoparticles decorated with CO_2H-terminated ligands increases their pK_a.[41] It should be possible, therefore, to trigger the rectifying state of SAMs of $S(CH_2)nCO_2H$ by exposure to a sufficiently strong acid.

Having already determined that aqueous acids have little impact on the magnitude of log|R|, we chose a merocyanine salt (MCH^+Cl^-) that is a relatively weak acid. Exposure to blue light induces a ring-closure to form spiropyran (SP) and HCl ($pK_a \approx -8$ in water). We chose MCH^+Cl^- in anhydrous ethanol because it is well-characterized[42] and has been shown to protonate CO_2H-terminated SAMs upon photoinduced ring-closure to SP.[29] The switching process and a schematic of the resulting protonation is shown in Figure 5a, and the resulting R/V data are shown in Figure 5b. Exposure to 1 mM ethanolic solutions of MCH^+Cl^- for 30 min has no effect on log|R| for $Au/S(CH_2)_{11}COOH//EGaIn$ junctions, indicating that the pK_a of MCH^+Cl^- in ethanol is too high to protonate CO_2H-terminated SAMs directly. With the addition of blue (350−450 nm) light, however, the junctions switch to the rectifying state, producing R/V curves that are almost indistinguishable from those that result from exposure to H_2O (Figure 1b). We attribute this result to the protonation of the terminal CO_2H groups by HCl, which can be thought of as $CO_2H{\cdot}HCl$ insofar as the rectifying behavior is the same as $CO_2H{\cdot}H_2O$ and the work function shifts downward by an additional 25 meV.

In conclusion, the ability to alter the function of a tunneling junction reversibly between resistor and diode creates the possibility of fabricating molecular-electronic devices that exhibit unique functions that are difficult or impossible to achieve with conventional semiconductor technology. Because rectification is self-referencing (i.e., it is independent of the

DOI: 10.1021/acs.nanolett.8b03042
Nano Lett. 2018, 18, 7552−7559

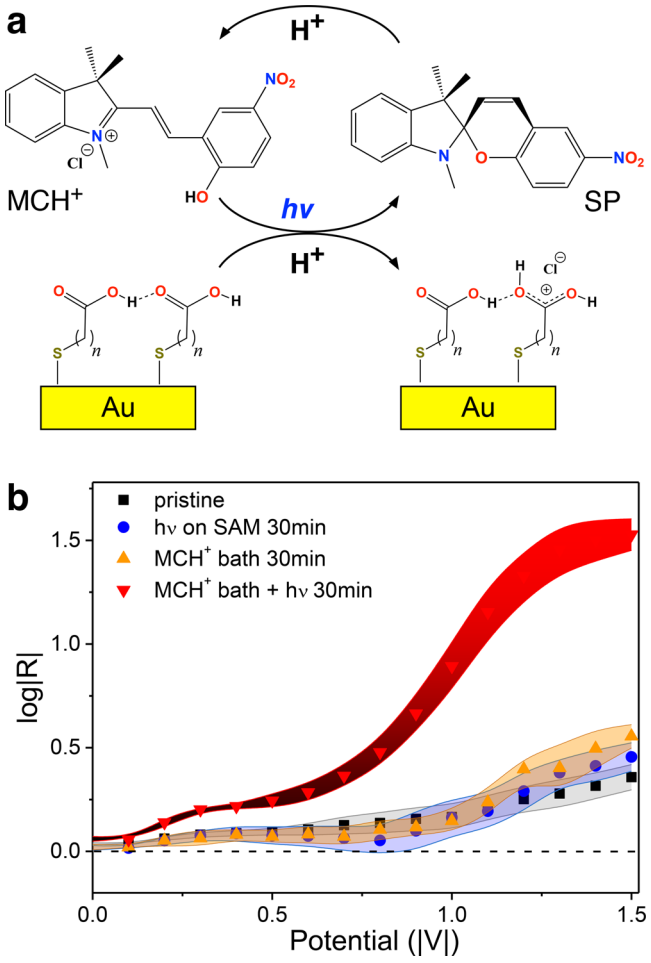

Figure 5. Converting between a nonrectifying and rectifying states using a photoacid. (a) When MCH^+Cl^-, a relatively weak acid, dissolved in anhydrous ethanol is exposed to blue (350−450 nm) light, it loses a proton and undergoes a reversible ring-closure to form SP, generating HCl, which is a sufficiently strong acid to protonate the CO_2H-terminated SAM, forming CO_2H·HCl. (b) Semilog plots of log|*R*| versus |*V*| for $Au^{TS}/S(CH_2)_{11}CO_2H//EGaIn$ junctions before and after the SAMs are exposed to MCH^+Cl^-, light ($h\nu$), or MCH^+Cl^- with light. Black, pristine; orange, exposure to $h\nu$ for 30 min; blue, exposure to 1 mM MCH^+Cl^- in anhydrous ethanol for 30; red, exposure to 1 MCH^+Cl^- in anydrous ethanol and $h\nu$ for 30 min.

absolute magnitude of *J*), rectification-modulation can potentially be used as a sensor or dosimeter. Although we used exposure to H_2O to characterize the effect and prove that it is molecular in nature, the XPS spectra and KPFM data suggest that the switching process is ultimately driven by the formation of a dipole moment when water binds the terminal CO_2H groups. Rectification can also be triggered by a strong acid, which can, in turn, be controlled with light or other inputs to produce devices with unique properties. For example, the function of a diode-logic circuit would depend on the outcomes of previous, proton-coupled events through the reversible switching of individual circuit elements; the magnitudes of log|*R*| in this work are already sufficient to create diode-logic circuits using EGaIn top-contacts.[5] There are myriad ways of delivering and transporting protons, and because the switching effect does not depend on the electrodes, proton-mediated rectification-modulation can potentially be both fast and robust with sufficient optimization in an appropriate device platform.

■ ASSOCIATED CONTENT

Supporting Information

The Supporting Information is available free of charge on the ACS Publications website at DOI: 10.1021/acs.nanolett.8b03042.

Details of junction measurements; Kelvin probe microscopy data; details of device fabrication; X-ray photoelectron spectroscopy; robustness study; individual *J*/*V* traces; control experiments; pH dependence study; and details of calculations (PDF)

■ AUTHOR INFORMATION

Corresponding Author

*E-mail: r.c.chiechi@rug.nl.

ORCID

Yanxi Zhang: 0000-0003-2622-8903

Kasper Nørgaard: 0000-0002-7784-7985

Ryan C. Chiechi: 0000-0002-0895-2095

Notes

The authors declare no competing financial interest.

■ ACKNOWLEDGMENTS

Y.A., A.K., Y.Z., and R.C.C. acknowledge the European Research Council for the ERC Starting Grant 335473 (MOLECSYNCON). X.Q. acknowledges the Zernike Institute for Advanced Materials "Dieptestrategie." K.N. acknowledges the Independent Research Fund Denmark Natural Sciences for the project "Getting in contact with molecules".

■ REFERENCES

(1) Service, R. F. The Brain Chip. *Science* **2014**, *345*, 614−616.

(2) Carlotti, M.; Kovalchuk, A.; Wächter, T.; Qiu, X.; Zharnikov, M.; Chiechi, R. C. Conformation-Driven Quantum Interference Effects Mediated by Through-Space Conjugation in Self-Assembled Monolayers. *Nat. Commun.* **2016**, *7*, 13904.

(3) Kumar, S.; van Herpt, J. T.; Gengler, R. Y. N.; Feringa, B. L.; Rudolf, P.; Chiechi, R. C. Mixed Monolayers of Spiropyrans Maximize Tunneling Conductance Switching by Photoisomerization at the Molecule−Electrode Interface in EGaIn Junctions. *J. Am. Chem. Soc.* **2016**, *138*, 12519−12526.

(4) Jia, C.; et al. Covalently Bonded Single-Molecule Junctions With Stable and Reversible Photoswitched Conductivity. *Science* **2016**, *352*, 1443−1445.

(5) Wan, A.; Suchand Sangeeth, C. S.; Wang, L.; Yuan, L.; Jiang, L.; Nijhuis, C. A. Arrays of High Quality SAM-based Junctions and Their Application in Molecular Diode Based Logic. *Nanoscale* **2015**, *7*, 19547−19556.

(6) Metzger, R. M. Unimolecular Electrical Rectifiers. *Chem. Rev.* **2003**, *103*, 3803−3834.

(7) Chen, X.; Roemer, M.; Yuan, L.; Du, W.; Thompson, D.; del Barco, E.; Nijhuis, C. A. Molecular Diodes With Rectification Ratios Exceeding 105 Driven by Electrostatic Interactions. *Nat. Nanotechnol.* **2017**, *12*, 797−803.

(8) Chiechi, R. C.; Weiss, E. A.; Dickey, M. D.; Whitesides, G. M. Eutectic Gallium−Indium (EGaIn): A Moldable Liquid Metal for Electrical Characterization of Self-Assembled Monolayers. *Angew. Chem.* **2008**, *120*, 148−150.

(9) Song, P.; Yuan, L.; Roemer, M.; Jiang, L.; Nijhuis, C. A. Supramolecular vs Electronic Structure: The Effect of the Tilt Angle of the Active Group in the Performance of a Molecular Diode. *J. Am. Chem. Soc.* **2016**, *138*, 5769−5772.

DOI: 10.1021/acs.nanolett.8b03042
Nano Lett. 2018, 18, 7552−7559

(10) Souto, M.; Yuan, L.; Morales, D. C.; Jiang, L.; Ratera, I.; Nijhuis, C. A.; Veciana, J. Tuning the Rectification Ratio by Changing the Electronic Nature (Open-Shell and Closed-Shell) in Donor−Acceptor Self-Assembled Monolayers. *J. Am. Chem. Soc.* **2017**, *139*, 4262−4265.
(11) Capozzi, B.; Xia, J.; Adak, O.; Dell, E. J.; Liu, Z.-F.; Taylor, J. C.; Neaton, J. B.; Campos, L. M.; Venkataraman, L. Single-Molecule Diodes With High Rectification Ratios Through Environmental Control. *Nat. Nanotechnol.* **2015**, *10*, 522−527.
(12) Atesci, H.; Kaliginedi, V.; Celis Gil, J. A.; Ozawa, H.; Thijssen, J. M.; Broek- mann, P.; Haga, M.-a.; van der Molen, S. J. Humidity-controlled rectification switching in ruthenium-complex molecular junctions. *Nat. Nanotechnol.* **2018**, *13*, 117−121.
(13) Clément, N.; Guérin, D.; Pleutin, S.; Godey, S.; Vuillaume, D. Role of Hydration on the Electronic Transport Through Molecular Junctions on Silicon. *J. Phys. Chem. C* **2012**, *116*, 17753−17763.
(14) Arnold, R.; Azzam, W.; Terfort, A.; Wöll, C. Preparation, Modification, and Crystallinity of Aliphatic and Aromatic Carboxylic Acid Terminated Self-Assembled Mono- layers. *Langmuir* **2002**, *18*, 3980−3992.
(15) Snow, A. W.; Jernigan, G. G.; Ancona, M. G. Packing density of HS(CH2)nCOOH self-assembled monolayers. *Analyst* **2011**, *136*, 4935−4949.
(16) Weiss, E. A.; Kaufman, G. K.; Kriebel, J. K.; Li, Z.; Schalek, R.; Whitesides, G. M. Si/SiO2-templated Formation of Ultraflat Metal Surfaces on Glass, Polymer, and Solder Supports: Their Use as Substrates for Self-Assembled Monolayers. *Langmuir* **2007**, *23*, 9686−9694.
(17) Li, D.; Mueller, M. B.; Gilje, S.; Kaner, R. B.; Wallace, G. G. Processable Aqueous Dispersions of Graphene Nanosheets. *Nat. Nanotechnol.* **2008**, *3*, 101−105.
(18) Muller, L.; Jacks, T. Rapid Chemical Dehydration of Samples for Electron Microscopic Examinations. *J. Histochem. Cytochem.* **1975**, *23*, 107−110.
(19) Carlotti, M.; Degen, M.; Zhang, Y.; Chiechi, R. C. Pronounced Environmental Effects on Injection Currents in EGaIn Tunneling Junctions Comprising Self-Assembled Monolayers. *J. Phys. Chem. C* **2016**, *120*, 20437−20445.
(20) Wimbush, K. S.; Fratila, R. M.; Wang, D.; Qi, D.; Liang, C.; Yuan, L.; Yakovlev, N.; Loh, K. P.; Reinhoudt, D. N.; Velders, A. H.; Nijhuis, C. A. Bias Induced Transition From an Ohmic to a Non-Ohmic Interface in Supramolecular Tunneling Junctions With Ga2O3/EGaIn Top Electrodes. *Nanoscale* **2014**, *6*, 11246−11258.
(21) Long, D. P.; Lazorcik, J. L.; Mantooth, B. A.; Moore, M. H.; Ratner, M. A.; Troisi, A.; Yao, Y.; Ciszek, J. W.; Tour, J. M.; Shashidhar, R. Effects of Hydration on Molecular Junction Transport. *Nat. Mater.* **2006**, *5*, 901−908.
(22) Zhang, X.; McGill, S. A.; Xiong, P. Origin of the Humidity Sensitivity of Al/AlO X/Mha/Au Molecular Tunnel Junctions. *J. Am. Chem. Soc.* **2007**, *129*, 14470−14474.
(23) Engelkes, V. B.; Beebe, J. M.; Frisbie, C. D. Length-Dependent Transport in Molecular Junctions Based on SAMs of Alkanethiols and Alkanedithiols: Effect of Metal Work Function and Applied Bias on Tunneling Efficiency and Contact Resistance. *J. Am. Chem. Soc.* **2004**, *126*, 14287−14296.
(24) Simeone, F. C.; Yoon, H. J.; Thuo, M. M.; Barber, J. R.; Smith, B.; Whitesides, G. M. Defining the Value of Injection Current and Effective Electrical Contact Area for EGaIn based Molecular Tunneling Junctions. *J. Am. Chem. Soc.* **2013**, *135*, 18131−18144.
(25) Weiss, E. A.; Chiechi, R. C.; Kaufman, G. K.; Kriebel, J. K.; Li, Z.; Duati, M.; Rampi, M. A.; Whitesides, G. M. Influence of Defects on the Electrical Characteristics of Mercury-Drop Junctions: Self-Assembled Monolayers of N-Alkanethiolates on Rough and Smooth Silver. *J. Am. Chem. Soc.* **2007**, *129*, 4336−4349.
(26) Cademartiri, L.; Thuo, M. M.; Nijhuis, C. A.; Reus, W. F.; Tricard, S.; Barber, J. R.; Sodhi, R. N. S.; Brodersen, P.; Kim, C.; Chiechi, R. C.; Whitesides, G. M. Electrical Resistance of Ag TS−S(CH 2) N-1CH 3//Ga 2O 3/EGaIn Tunneling Junctions. *J. Phys. Chem. C* **2012**, *116*, 10848−10860.
(27) Huang, Y.-L.; Tien, H.-W.; Ma, C.-C. M.; Yang, S.-Y.; Wu, S.-Y.; Liu, H.-Y.; Mai, Y.-W. Effect of Extended Polymer Chains on Properties of Transparent Graphene Nanosheets Conductive Film. *J. Mater. Chem.* **2011**, *21*, 18236−18241.
(28) Kim, J.; Yamada, Y.; Kawai, M.; Tanabe, T.; Sato, S. Spectral Change of Simulated X-Ray Photoelectron Spectroscopy From Graphene to Fullerene. *J. Mater. Sci.* **2015**, *50*, 6739−6747.
(29) Kundu, P. K.; Samanta, D.; Leizrowice, R.; Margulis, B.; Zhao, H.; Börner, M.; Udayabhaskararao, T.; Manna, D.; Klajn, R. Light-Controlled Self-Assembly of Non- Photoresponsive Nanoparticles. *Nat. Chem.* **2015**, *7*, 646−652.
(30) Akkerman, H. B.; Blom, P. W. M.; de Leeuw, D. M.; de Boer, B. Towards Molecular Electronics With Large-Area Molecular Junctions. *Nature* **2006**, *441*, 69−72.
(31) Puebla-Hellmann, G.; Venkatesan, K.; Mayor, M.; Lörtscher, E. Metallic nanoparticle contacts for high-yield, ambient-stable molecular-monolayer devices. *Nature* **2018**, *559*, 232−235.
(32) Tu, A.; Kwag, H. R.; Barnette, A. L.; Kim, S. H. Water Adsorption Isotherms on CH3-, OH-, and COOH-terminated Organic Surfaces at Ambient Conditions Measured With PM-RAIRS. *Langmuir* **2012**, *28*, 15263−15269.
(33) Morales, G. M.; Jiang, P.; Yuan, S.; Lee, Y.; Sanchez, A.; You, W.; Yu, L. Inversion of the Rectifying Effect in Diblock Molecular Diodes by Protonation. *J. Am. Chem. Soc.* **2005**, *127*, 10456−10457.
(34) Kovalchuk, A.; Egger, D. A.; Abu-Husein, T.; Zojer, E.; Terfort, A.; Chiechi, R. C. Dipole-Induced Asymmetric Conduction in Tunneling Junctions Comprising Self- Assembled Monolayers. *RSC Adv.* **2016**, *6*, 69479−69483.
(35) Qiu, L.; Zhang, Y.; Krijger, T. L.; Qiu, X.; van't Hof, P.; Hummelen, J. C.; Chiechi, R. C. Rectification of Current Responds to Incorporation of Fullerenes Into Mixed-Monolayers of Alkanethiolates in Tunneling Junctions. *Chem. Sci.* **2017**, *8*, 2365−2372.
(36) Kong, G. D.; Kim, M.; Cho, S. J.; Yoon, H. J. Gradients of Rectification: Tuning Molecular Electronic Devices by the Controlled Use of Different-Sized Diluents in Heterogeneous Self-Assembled Monolayers. *Angew. Chem., Int. Ed.* **2016**, *55*, 10307−10311.
(37) Nijhuis, C.; Reus, W. F.; Barber, J. R.; Dickey, M. D.; Whitesides, G. M. Charge Transport and Rectification in Arrays of SAM-Based Tunneling Junctions. *Nano Lett.* **2010**, *10*, 3611−3619.
(38) Xie, Z.; Bâldea, I.; Frisbie, C. D. Why one can expect large rectification in molecular junctions based on alkane monothiols and why rectification is so modest. *Chem. Sci.* **2018**, *9*, 4456−4467.
(39) Ottosson, N.; Wernersson, E.; Söderström, J.; Pokapanich, W.; Kaufmann, S.; Svensson, S.; Persson, I.; Öhrwall, G.; Björneholm, O. The protonation state of small carboxylic acids at the water surface from photoelectron spectroscopy. *Phys. Chem. Chem. Phys.* **2011**, *13*, 12261−12267.
(40) Kakiuchi, T.; Iida, M.; Imabayashi, S.-i.; Niki, K. Double-Layer-Capacitance Titra- tion of Self-Assembled Monolayers of Ω-Functionalized Alkanethiols on Au(111) Surface. *Langmuir* **2000**, *16*, 5397−5401.
(41) Wang, D.; Nap, R. J.; Lagzi, I.; Kowalczyk, B.; Han, S.; Grzybowski, B. A.; Szleifer, I. How and Why Nanoparticle's Curvature Regulates the Apparent P Kaof the Coating Ligands. *J. Am. Chem. Soc.* **2011**, *133*, 2192−2197.
(42) Klajn, R. Spiropyran-Based Dynamic Materials. *Chem. Soc. Rev.* **2014**, *43*, 148−184.

■ NOTE ADDED AFTER ASAP PUBLICATION

This paper published ASAP on 11/9/2018. The spelling of a surname in the author list was corrected and the revised version was reposted on the same day.

DOI: 10.1021/acs.nanolett.8b03042
Nano Lett. 2018, 18, 7552−7559